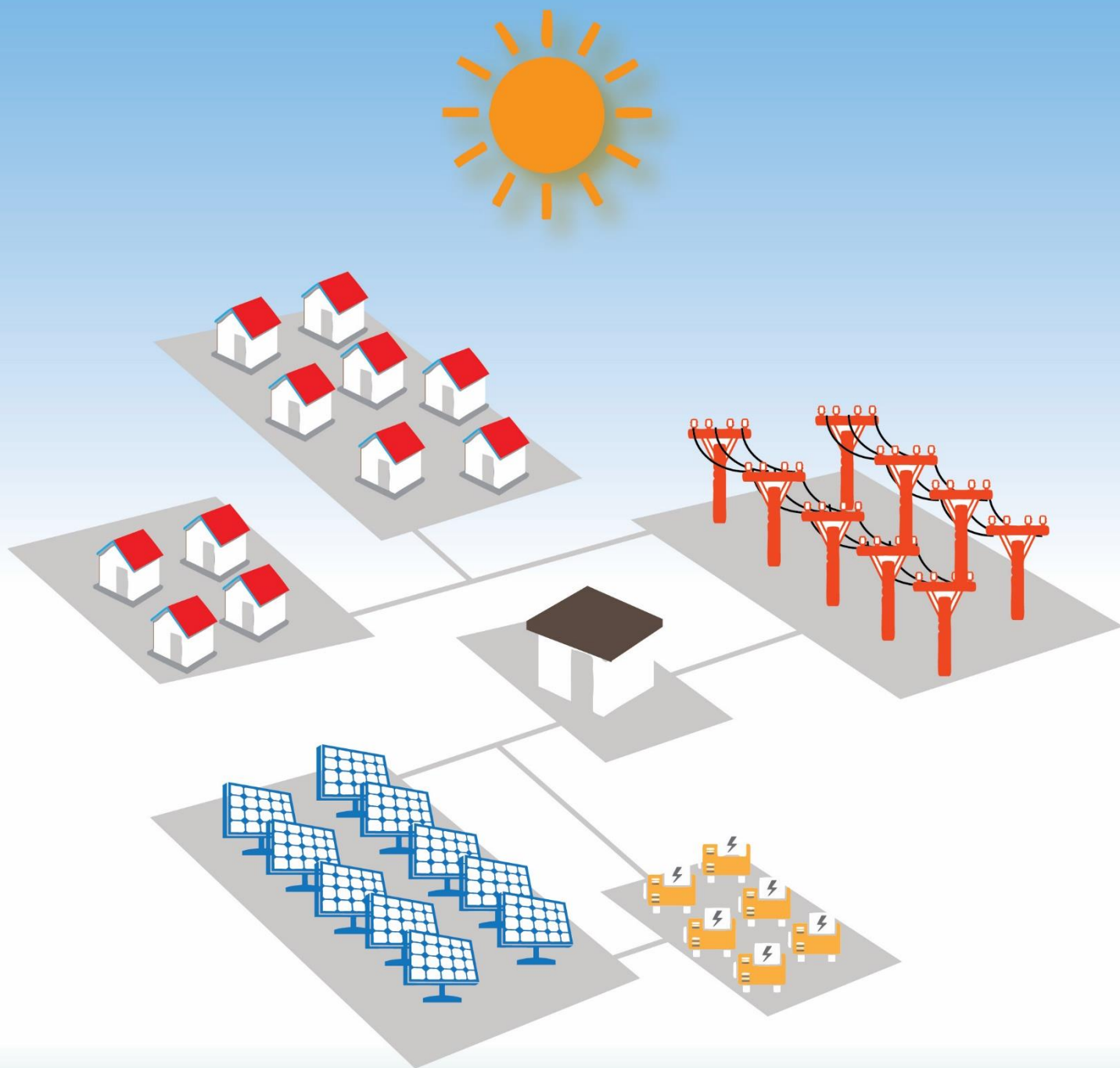


# Techno-Economic Analysis of Stand-alone Solar PV and Battery based Micro-grids in Karnataka





# **Techno-Economic Analysis of Stand-alone Solar PV and Battery based Micro-grids in Karnataka**

Vaishalee Dash

Badri S. Rao

Harshid Sridhar

Dr Mridula D. Bharadwaj

**Center for Study of Science, Technology and Policy  
June, 2018**

Center for Study of Science, Technology and Policy (CSTEP) is a private, not-for-profit (Section 25) Research Corporation registered in 2005.

Designing and Editing by CSTEP

Disclaimer

While every effort has been made for the correctness of data/information used in this report, neither the authors nor CSTEP accept any legal liability for the accuracy or inferences for the material contained in this report and for any consequences arising from the use of this material.

© 2018 Center for Study of Science, Technology and Policy (CSTEP)

This report is a part of the Indo-US collaborative research platform – Solar Energy Research Institute for India and the United States (SERIUS). No part of this report may be disseminated or reproduced in any form (electronic or print) without permission from CSTEP or SERIUS consortium.

This report should be cited as: CSTEP, (2018). *Techno-Economic Analysis of Stand-alone Solar PV and Battery based Micro-grids in Karnataka*, (CSTEP-Report-2018-09).

June, 2018  
Center for Study of Science, Technology and Policy  
# 18, 10th Cross, Mayura Street,  
Papanna Layout, Nagashettyhalli, RMV II Stage,  
Bangalore-560094 Karnataka, INDIA  
Tel.: +91 (80) 6690-2500  
Fax: +91 (80) 2351-4269  
Email: [cpe@cstep.in](mailto:cpe@cstep.in)  
Website: [www.cstep.in](http://www.cstep.in)



## Foreword

It is not an understatement to say that the economy of a country runs on energy. In fact, if there is one parameter that correlates most directly and tangibly with economic growth, it is the availability of adequate energy. On the flip side, economic poverty and energy poverty go hand in hand. Access to energy has proven to be a key determinant of several enablers of development; most notably, improved outcomes in education, primary health, gender empowerment and livelihoods.

For a country like India, with its vast geographical spread, providing access to affordable electricity to every household has been a challenge, especially in remote rural areas. This has been slowly but surely changing, and in the last few years, rural electrification in India has made good progress. Both the central and state governments have been giving high priority to last-mile electrification with the result that today almost every village has a connection to the grid. However, the challenge still remains in ensuring that every household in every village gets access to affordable power. The recently launched Saubhagya scheme by Government aims to bridge the gap between 100% electrification of villages and 100% electrification of households.

The challenges of rural electrification through grid extension are many; primarily the high cost of supplying power and the low revenue returns— often in combination with lower demand for electricity. In addition, the unsatisfactory financial state of most distribution companies makes it very difficult for them to consider rural regions as a viable consumer market. Progress in rural electrification has therefore depended heavily on direct government support.

In the face of these challenges, the question before us is: “Is there a viable alternative model of providing energy access to rural areas?”

This is where the promise of renewable energy comes in, especially its off-grid and micro-grid versions. If designed and deployed properly, decentralised renewable power systems can play a significant role in plugging the gaps in India’s electrification story. The strong momentum in solar power combined with its decreasing cost makes off-grid solar technologies an exciting option. It can also augment the productive use of energy in agriculture and in village level micro-enterprises, thus galvanising a virtuous cycle of development and improved quality of life in rural communities.

But what is needed to make this happen? Can off-grids and micro-grids work in all situations and scenarios? If not, what are the pre-requisites and conditions necessary to make it work? These questions are of critical systemic importance.

At Wipro, our work in social initiatives is driven by the need to engage deeply and understand such systemic issues, whether in energy, water or education. For this purpose, we work with partners who have a deep understanding of the respective domain and whose values are aligned with ours. CSTEP with its deep expertise and competence in the areas of energy and climate change is a natural choice as a partner in this space.

Registered Office:

**Wipro Limited**  
Doddakannelli  
Sarjapur Road  
Bengaluru 560 035  
India

T : +91 (80) 2844 0011  
F : +91 (80) 2844 0054  
E : [info@wipro.com](mailto:info@wipro.com)  
W : [wipro.com](http://wipro.com)  
C : L32102KA1945PLC020800







This report from CSTEP provides a robust techno-economic methodology to help design and size solar photovoltaic and battery based off-grid micro-grids that allow local generation and supply of power in rural communities. The role of system dispatch, especially in the trade-off between cost and reliability of power supply has been highlighted in the report. The study also shows the importance of having granular data in modelling system operation, and its impact on system cost. The analysis is based on villages in Karnataka. However, the methodology can be applied to evaluate any rural region in India.

I hope this study finds interest among various stakeholders such as researchers, policy-makers, academia and industry in understanding micro-grid system design and associated techno-economics.

I congratulate the CSTEP team for their commitment, competence and diligence in completing this comprehensive and insightful study and wish them continued success in their future endeavours.

A handwritten signature in blue ink, appearing to read "P.S. Narayan".

P.S. Narayan

Vice President and Head – Sustainability

Wipro Ltd



Registered Office:

Wipro Limited  
Doddakannelli  
Sarjapur Road  
Bengaluru 560 035  
India

T : +91 (80) 2844 0011  
F : +91 (80) 2844 0054  
E : info@wipro.com  
W : wipro.com  
C : L32102KA1945PLC020800



## Executive Summary

Access to electricity can bring about a transformative change in the economic conditions and growth of any country. It not only helps in improving the living conditions of the society at large, but also provides them with ample revenue opportunities to earn a livelihood. In India, the lack of electricity supply has affected the rural regions in many ways, including quality of life, agriculture and economic growth. Currently, close to three crore households are still awaiting access to electricity.

Decentralised solar energy solutions like solar lanterns, solar home lighting systems, rooftop Photovoltaic (PV) systems, and solar micro-grids and mini-grids have been in use for quite some time. In this study, for select sites considered in Karnataka, we analysed the feasibility of Solar PV Micro Grids (SPVMGs), considering its potential as a promising solution for electrifying rural homes and villages. SPVMGs can easily facilitate local generation and distribution of power, without relying on the central power grid.

We conducted a detailed techno-economic analysis of a SPVMG. Broadly, the analysis revealed that the cost of generating and supplying power from a SPVMG, for the sites considered in Karnataka, is in the range of INR 31–34/kWh, which is much higher than the retail electricity rates in India. This suggests that SPVMGs can be an ideal solution when the cost of electricity supply through grid extension exceeds the cost of electricity from SPVMGs. We also observed that trading off between cost and reliability of supply is essential in stand-alone (off-grid) SPVMGs. Restricting the battery discharge to 12 hours (between 6 PM to 6 AM) provides reasonably good reliability at slightly lower Levelised Cost of Electricity (LCOE), as compared to allowing  $24 \times 7$  discharge of battery.

Key aspects of the study included simulating the generation characteristics of a SPVMG; calculating the battery life based on different dispatch strategies; and conducting a scenario analysis to help find a suitable or close-to-optimal system configuration. A financial model, developed for SPVMG analysis, was used to evaluate the economic feasibility of technically appropriate system sizes.

We carried out a system sizing study to determine the appropriate size of a SPVMG by trading off between cost and reliability of supply. We analysed different scenarios by simulating a dispatch logic, which varied the maximum hours of battery discharge from 6 and 12 hours to 24 hours. In a scenario where a battery discharges for 12 hours (between 6 PM to 6 AM), the system reliability is reasonably good (approximately 21 hours of supply) and the LCOE is comparable to those in the other two scenarios, i.e., 6 and 24 hours of battery discharge. The 12 hour battery discharge scenario provides a good trade-off between cost and reliability, hence we call it the “balanced” scenario, in this report. We performed sensitivity analyses for the system size obtained in the “balanced” scenario to further understand the scope of cost reduction.

The approach used in this study enables one to achieve a trade-off between cost and reliability for a SPVMG. It also reveals the importance of the dispatch strategy for optimising battery operation and its size, by ensuring that the battery is neither oversized for high system reliability, nor undersized to reduce system cost. Moreover, the study highlighted the significance of performing minute-wise simulations for a detailed understanding of system operation.

## Acknowledgements

The authors would like to express their gratitude to WIPRO for supporting CSTEP's work on issues related to energy access. We would especially like to thank Mr P.S. Narayan, Vice President and Head of Sustainability and Social Initiatives, WIPRO, for his valuable feedback and comments during the project reviews.

We are thankful for the immense support received from Sh. P. Ravikumar, Additional Chief Secretary and Sh. Rajkumar S. Biradar, Joint Director, from the Energy Department, Government of Karnataka for facilitating data requirements for the project. We would also like to express our gratitude to the officials in the State Load Despatch Centre (SLDC), especially Sh. S.B. Chandrasekharaiah, Executive Engineer, SLDC Karnataka, for helping us with the data needed for the study.

We would like to thank our CSTEP colleagues Dr Bellarmine K.C. for his valuable suggestions regarding the analysis; Dr Parveen Kumar for advising us during the course of the project; Aklavya Sharan for sharing practical insights on solar micro-grid operation; and Ravi Lepakshi for providing insights on typical village electrification projects in Karnataka. We are also thankful to Rushil Zutshi for his valuable contribution to the project during his summer internship at CSTEP in 2016.

We are grateful to Dr S.S. Krishnan (Advisor), Thirumalai N.C. (Principal Research Scientist), Dr Jai Asundi (Research Coordinator) and Dr Anshu Bharadwaj (Executive Director), from CSTEP, for their comprehensive feedback and suggestions regarding the report. In addition, we thank Merlin Francis, Arushi Sen, Abhijit Chakraborty and Aswathy Shivaji for providing editorial support and graphics inputs.

This work was further supported, in part, by the US-India Partnership to Advance Clean Energy-Research (PACE-R) for the Solar Energy Research Institute for India and the United States (SERIUS), funded jointly by the U.S. Department of Energy (Office of Science, Office of Basic Energy Sciences, and Energy Efficiency and Renewable Energy, Solar Energy Technology Program, under Subcontract DE-AC36-08G028308 to the National Renewable Energy Laboratory, Golden, Colorado) and the Government of India, through the Department of Science and Technology under Subcontract IUSSTF/JCERDC-SERIUS/2012 dated 22nd November, 2012.



## Table of Contents

1. Introduction .....	1
1.1 System Configuration .....	2
2. Methodology for Techno-Economic Analysis of SPVMG .....	3
2.1 Overview of Methodology .....	3
2.2 Site Selection .....	4
2.3 Inputs for the Analysis .....	5
3. Modelling of SPVMG .....	6
3.1 Solar PV Modelling .....	6
3.2 Battery Storage Modelling.....	8
3.3 Technical Modelling for SPVMG.....	12
3.4 Financial Modelling for SPVMG.....	13
3.5 Techno-economic Modelling for SPVMG .....	14
4. Results and Discussion .....	15
4.1 Typical System Performance.....	15
4.2 Scenarios for Feasibility Analysis.....	17
4.3 System Costs .....	20
4.4 Sensitivity Analysis .....	22
4.5 Techno-economic Comparison for Hourly and Minute-wise Simulations .....	22
5. Policy Implications and Way Forward.....	24
References .....	25
Appendix A.....	26

## List of Figures

Figure 1: Block schematic of the SPVMG system configuration .....	3
Figure 2: Block schematic for SPVMG design and simulation .....	4
Figure 3: Block schematic for the lead-acid battery model .....	9
Figure 4: Sample SoC data and filtered SoC for rain flow counting algorithm .....	12
Figure 5: PV and battery performance characteristics over five typical days .....	16
Figure 6: Variation in (a) reliability indicators and (b) battery life and efficiency for a 35 kW PV system .....	17
Figure 7: Scenarios 1-3 showing the variation in system unmet load .....	17
Figure 8: Variation in system LCOE for Scenarios 1-3 .....	18
Figure 9: Break-up of capital cost and fixed cost for the “balanced” system .....	21
Figure 10: Break-up of capital cost for the “balanced” system .....	21
Figure 11: Break-up of fixed cost for the “balanced” system .....	21
Figure A.1.1: Typical load demand for representative days in four different months .....	27

## List of Tables

Table 1: Initial list of shortlisted villages .....	4
Table 2: SRRRA station and solar data specifications .....	6
Table 3: System losses considered in solar PV output power modelling .....	7
Table 4: Inputs for the battery performance model .....	9
Table 5: Battery dispatch Scenarios .....	11
Table 6: Input system cost for a typical SPVMG .....	13
Table 7: O&M expenses .....	13
Table 8: Parameters for project finance .....	14
Table 9: System configurations w.r.t. lower LCOE and higher reliability .....	19
Table 10: System configurations obtained by trading-off both LCOE and unmet load .....	20
Table 11: Break-up of capital and fixed costs for the “balanced” system .....	20
Table 12: Break-up of capital cost for the “balanced” system .....	20
Table 13: Break-up of fixed cost for the “balanced” system .....	21
Table 14: Break-up of “balanced” system cost with grant based funding .....	22
Table 15: Break-up of “balanced” system cost using VRLA Gel battery .....	22
Table 16: Techno-economic comparison of hourly and minute-wise simulations for the “balanced” system .....	23
Table A.1.1: Use of electricity in a typical village in India .....	27
Table A.2.1: Solar PV module datasheet parameters .....	28

## 1. Introduction

Electrical energy can transform and uplift the socio-economic condition of a region—this is a well-established fact (Jain et al., 2015). By November 2017, India's Grameen Vidyutikaran (GARV) dashboard indicated that 82% of the targeted village electrification work had been achieved (Rural Electrification Corporation, 2017). In April 2018, the Government of India released a statement to announce that 100 % electrification had been achieved for India. However, this translates to about 3.1 crore households still waiting for electricity connections, indicating a long road ahead for the country in achieving 100% electrification<sup>1</sup>. A large section of the population continues to live in areas that receive deficient supply—no more than an average of 6 hours a day (Jain et al., 2015).

Rural electrification in India has been a subject of debate for many years. This has also been an area of keen interest for every elected government. Both the central and state governments have launched numerous programmes and schemes to promote and support the cause. One of the largest rural electrification programmes launched by the Centre was the Rajiv Gandhi Grameen Vidyutikaran Yojana (RGGVY) in 2005. The recent Deen Dayal Upadhyay Gram Jyoti Yojana (DDUGJY), launched in 2015, subsumed RGGVY. Various government bodies have heavily subsidised the cost of rural electrification in the past. Under DDUGJY, the Ministry of Power (MoP) provides a maximum of 75% grant for projects in general states and up to 90% funding for special states (all North-eastern states, including Sikkim, Jammu & Kashmir, Himachal Pradesh and Uttarakhand).

The progress made so far is reasonable considering some of the challenges associated with the sector. People's inability to pay for electricity has historically been one of the main reasons for lack of power supply in villages. In order to reduce retail electricity rates for villages, the government cross-subsidises the cost with bulk urban consumers. Another challenge to rural electrification is that Distribution Companies (DISCOMs) find it expensive to extend and maintain grid infrastructure in remote rural areas. The high Aggregate Technical and Commercial (AT&C) losses and resultant poor financial state of the DISCOMs also deter rural electrification.

However, with millions of people still living in darkness and extreme poverty, access to electricity would be a massive enabler in improving their quality of life; solutions to make this possible must be explored. While India has witnessed a dramatic reduction in bid prices for large-scale Photovoltaic (PV) projects<sup>2</sup>, primarily due to the low cost of PV modules, very little has been done to utilise this opportunity to promote solar PV for rural electrification. The higher cost of transporting equipment to remote regions; the cost of building distribution infrastructure; and a lack of focus on promoting such off-grid and decentralised solar technologies under the National Solar Mission have caused this sector to underperform, as compared to utility scale solar.

Off-grid solar technologies have their own advantages. Such solutions allow local generation and consumption of power, thereby reducing transmission losses, in remote regions. One such example is the Solar PV Micro Grid (SPVMG), which comprises PV modules and a battery-

---

<sup>1</sup> <https://thewire.in/government/narendra-modi-government-rural-electrification-power>

<sup>2</sup> <http://www.livemint.com/Industry/zW5Lf1okn054cFug5yKGsL/Madhya-Pradesh-solar-bids-hovering-at-Rs3-per-unit-in-revers.html>

backed system. It can be a potential solution for powering rural communities and eliminating the need for extending the grid to remote, far-flung areas.

Till date, the private sector has majorly contributed in deploying off-grid solar installations in India. Most projects were initiated through Corporate Social Responsibility (CSR) grants, individual equity contributions, foreign grants or government subsidies. These private Renewable Energy Supply Providers (RESPs) execute end-to-end micro-grid projects, including laying out the Public Distribution Network (PDN) and connecting all households. A suitable tariff, based on the project cost, is collected from the village every month. The tariff for such a SPVMG is typically high as compared to utility electricity rates, but prevents these rural households from the inconvenience and cost of using kerosene or diesel for lighting and other uses. However, this sector is largely unregulated and there is no overarching policy to provide direction, till date<sup>3</sup>. RESPs today, primarily supply lighting loads, and some of them also connect pumps for irrigation or drinking water supply. However, the supply is largely restricted, using load limiters, as it becomes difficult to manage sudden demand surges from the consumer's end, especially in an off-grid set-up.

The objective of this study was to carry out a techno-economic feasibility analysis for SPVMGs in the rural areas of Karnataka (KA). For this, it was important to understand the system size requirements and cost for a SPVMG. We carried out the sizing analysis considering actual site load demand profiles, using data from electricity feeders in rural KA. We considered polycrystalline PV and Valve-Regulated Lead-Acid (VRLA) battery technology in the study. In the analysis, we modelled PV and battery performance and estimated battery life using a cycle-counting algorithm, instead of relying on manufacturer-specified battery life. We used this to calculate the battery replacement costs more realistically in our financial calculations. We performed a techno-economic analysis by considering three different scenarios. This helped us in successfully identifying a "balanced" scenario, which provides a system with a reasonable LCOE and fairly good system reliability as compared to the other two scenarios. In Sections 2–5 of the report, we discuss, the system configuration, methodology, modelling approach, results and conclusions of the study.

## 1.1 System Configuration

The system configuration for the analysis (Figure 1) considers solar PV as the main source of power for the load demand. The PV power is prioritised to supply the load first, before charging the battery during excess generation. During periods of no solar generation or high demand, the battery discharges to meet the load.

---

<sup>3</sup> A draft policy for mini-grids was released in 2016, but has not reached the final stage of approval

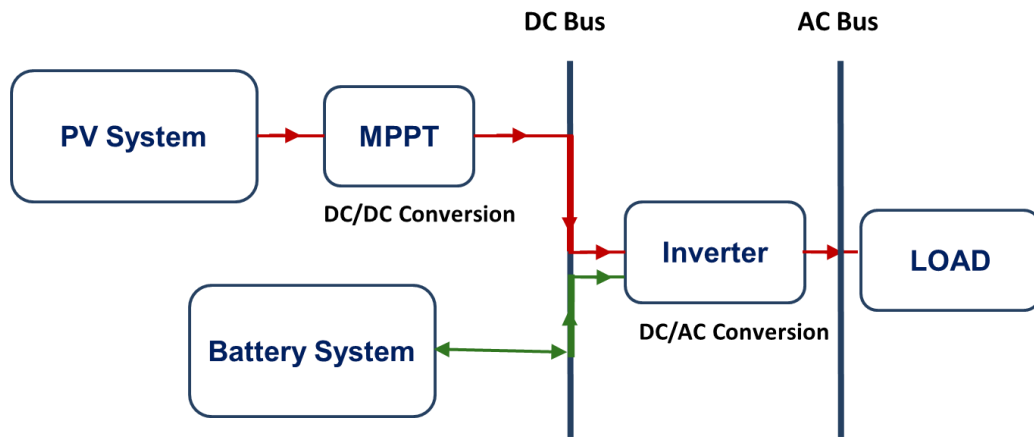


Figure 1: Block schematic of the SPVMG system configuration

The solar PV system, along with a battery, is connected to the Direct Current (DC) side of the inverter. A Maximum Power Point Tracking (MPPT) charge controller charges the battery and ensures that the battery charging power and bus voltage are within specified limits. The inverter converts DC solar power into Alternating Current (AC), to supply the load directly. Similarly, the battery power, during discharge, is routed through the inverter for AC conversion. A few manufacturers embed the MPPT feature in the inverter. Although we have considered both DC/DC and DC/AC conversion efficiencies for conservative power calculations, we have only assumed a single cost for the charge controller and inverter set in the financial calculations.

## 2. Methodology for Techno-Economic Analysis of SPVMG

In this section, we briefly discuss the methodology used for carrying out a detailed techno-economic analysis of a SPVMG. It includes an overview of the methodology; and a description of the pre-requisites for the techno-economic analysis such as site selection and inputs required for the analysis. In the next section, we elaborate on the system modelling approach.

### 2.1 Overview of Methodology

The framework developed for this study identified the appropriate system size. It constituted a set of inputs, dispatch model and outputs in the form of reliability indicators. In order to calculate the PV size ( $PV_s$ ) and battery size ( $BAT_s$ ) for the various dispatch scenarios, we used different combinations of PV and battery capacities, in an iterative manner, as inputs to the PV and battery models. The PV and battery power outputs were subsequently passed to the dispatch model. The dispatch model then calculated reliability indicators such as unmet load ( $UL$ ), excess electricity ( $EX_{EL}$ ) and loss of power supply probability ( $T_{LPSP}$ ). The load demand profile remained the same for all the simulated scenarios. Figure 2 presents a block schematic of the interaction between system inputs and reliability indices for a typical SPVMG dispatch scenario.



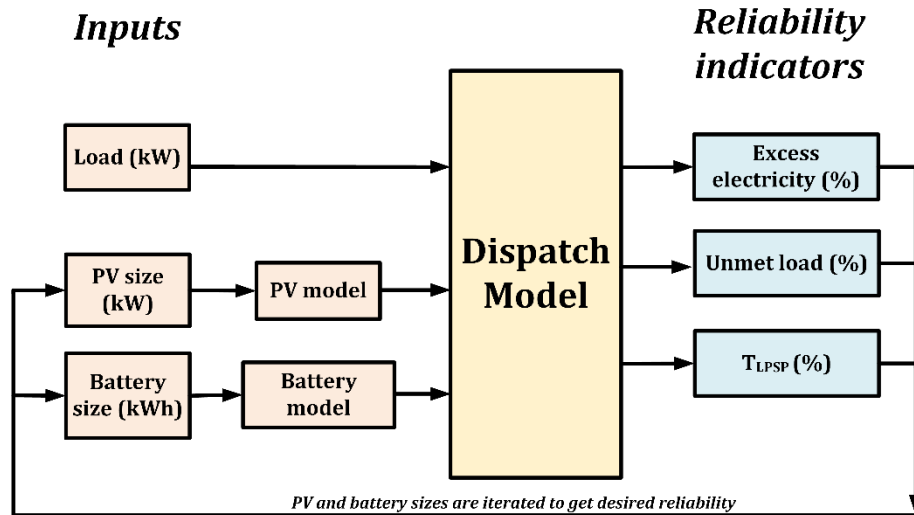


Figure 2: Block schematic for SPVMG design and simulation

For each combination of PV and battery, the system LCOE along with reliability parameters were recorded. Finally, we sorted the systems based on the lowest LCOE and unmet load (high reliability). Various dispatch scenarios were tested and a “balanced” system, in terms of both cost and reliability, was chosen as the final system configuration.

## 2.2 Site Selection

We selected sites for the study based on the criteria mentioned below:

- The villages or sites should be un-electrified
- They should have close proximity to Solar Radiation Resource Assessment (SRRA) ground stations, deployed by the National Institute of Wind Energy (NIWE)
- Real load data from neighbouring sites should be available.

Since a SPVMG is well-suited for un-electrified sites, an important pre-requisite for the study was to identify un-electrified villages in KA. We used information available on the GARV dashboard for initially screening potential sites. The dashboard provides details of electrification based on grid extension or off-grid plans. According to the data available on the dashboard in May 2016, 28–30 villages in Hassan, Shimoga and Chamarajanagar districts fell within the scope of this project. Since the study involved modelling of solar PV characteristics to estimate generation, access to good-quality ground solar data was important. Thus, we had to consider a site’s proximity to SRRA stations set up by NIWE. Sites that were less than 100 km from the periphery of SRRA stations, were first selected. As it turned out, all shortlisted sites satisfying the criteria were in the Chamarajanagar district. Table 1 shows a list of all the shortlisted sites.

Table 1: Initial list of shortlisted villages

District	Block	Village	SRRA Station
Chamarajanagar	Chamarajanagar	Bedaguli	Erode
	Kollegal	Bellaji Beat	Mysore
	Kollegal	Indiganatha A Beat	Erode
	Kollegal	Indiganatha B Beat	Erode
	Kollegal	Palar Beat	Erode

The load demand data is another important input for the model and crucial for site selection. We required load data to perform system sizing and determine the capacity of the potential PV plant, battery and inverter. For un-electrified villages, the demand data are typically generated based on the energy needs of the village. A field survey is conducted by the project developer, at times, to estimate the current and future need for electricity. However, in this study, our aim was to determine the SPVMG size, considering a demand pattern similar to or closely resembling an actual rural demand pattern. The reason behind this was to understand the system capacity requirements for catering to the real rural demand, similar to what the proposed site would see in the future. This is contrary to the approach followed by most micro-grid developers today, where the system is typically designed to provide a pre-decided quantum of energy, with limited consideration for future growth in load demand.

We approached the Energy Department of the Government of Karnataka for consultation regarding demand data. Based on our discussions, we considered the demand data from the 11 kV feeders close to the shortlisted sites as input for the sizing analysis. The 11 kV feeder data represented the aggregated load demand for a cluster of villages. This data-set from the neighbouring electrified villages provided a realistic estimate of the pattern of electricity consumption in that region, hence we used it in the study. We obtained minute resolution data from select feeders through a formal request to the Karnataka State Load Despatch Centre (SLDC). The SLDC data included active power consumption data at a minute-level time scale for the period January–December, 2015, for the two feeders closest to the chosen villages. Feeder F2 was the representative feeder for Bedaguli. The other feeder (F6), between Cowdalli substation and Male Mahadeswara hills, was representative for the remaining villages, namely Bellaji Beat, Indiganatha A Beat, Indiganatha B Beat and Palar Beat.

A visual inspection of the data revealed that for the period under consideration (January–December, 2015), the quality of data for feeder F6 was comparatively superior to that of feeder F2. Thus, we found the villages in the Kollegal block of Chamarajanagar district (represented by feeder F6), i.e., Bellaji Beat, Indiganatha A Beat, Indiganatha B Beat and Palar Beat, to be suitable. However, we finally selected all villages except Bellaji Beat for the study because the solar resource data for these three sites could be mapped from a single SRRRA station (Erode), which is located at a distance of approximately 90 km from the sites.

## 2.3 Inputs for the Analysis

Two crucial inputs, namely load demand data and solar irradiance and weather data, were needed for conducting the analysis. While the first one was needed to help design the SPVMG and determine individual component sizes, the second one was needed to model the solar PV power output.

### 2.3.1 Load demand data

We found the demand data from feeder F6 to be the most suitable for the study, as explained in Section 2.2. This data-set had 83,321 zero-value points, out of the total 5,25,600 values, representing minute-level resolution data for one year. These points indicated missing data, and those corresponding to load shedding instants. In order to perform a thorough system sizing study, we needed a continuous demand profile. We used a data averaging technique to obtain a continuous demand profile, capturing fluctuations in power, without disturbing the data trends. In addition, we used a scaling approach to determine a representative load profile for the analysis. The scaled-down profile had a peak demand of 14 kW, which is similar to the

peak electricity demand seen in typical Indian villages, comprising around 120–130 households. The details of the calculation are described in Appendix A.1.

### 2.3.2 Solar radiation data

The solar radiation data, procured from NIWE, had close to 42,928 missing data points, out of a total 5,25,600 points, depicting an entire year's data. We interpolated these data points linearly to form a continuous solar resource profile. This was crucial for performing the sizing analysis, where solar generation and demand had to be compared, to determine the contribution of PV and battery in meeting the demand. We identified the data points, which formed the boundary of the bad data subsets, and linearly interpolated them using the two point line equation.

If “ $t$ ” is the reference minute of a day (1 to 1,440), then “ $P_M(t)$ ” is the corresponding module power output for that instant. We used the equation mentioned below to interpolate between  $(t_1, P_{M1})$  and  $(t_2, P_{M2})$ , as the two boundary points of interest:

$$P_M(t) = t * \left[ \frac{P_{M2} - P_{M1}}{t_2 - t_1} \right] - t_1 * \left[ \frac{P_{M2} - P_{M1}}{t_2 - t_1} \right] + P_{M1}$$

## 3. Modelling of SPVMG

In order to perform a techno-economic modelling of a SPVMG, it was crucial to model the power generation characteristics of the solar PV and battery to determine the power output of the combined system. Once the technical model was built to simulate the generation characteristics, we also prepared a financial model for the micro-grid. Outputs from individual models, when combined, provided insights on the system viability.

### 3.1 Solar PV Modelling

The PV modelling exercise helped to determine the exact quantum of power generated for an input PV size, based on the site solar resource data. As mentioned in Section 2.2, we mapped the selected villages to a single SRRRA station, i.e., Erode in Tamil Nadu. We procured the solar resource data (1 minute resolution) for Erode from NIWE. Table 2 describes the details of the SRRRA station and the data availability period (National Institute of Wind Energy, 2017).

Table 2: SRRRA station and solar data specifications

SRRRA and Solar Data Details	
Location	Erode
Latitude [°N]	11.27
Longitude [°E]	77.6
Altitude [m]	272
Period From	01-11-14, 0:01
Period To	01-11-15, 0:00

First, we modelled the PV generation profile for 1 kWp capacity, using a 320 Wp polycrystalline module from Vikram Solar as reference, to extract the module parameters (for more details, refer Appendix A.2). We then scaled up this base profile of 1 kW to calculate

generation for higher PV capacities. The generation profile from the PV model refers to the Direct Current (DC) output power of the solar PV.

The list below describes the assumptions used in PV modelling:

- The plant has a fixed tilt configuration, with module tilt equal to the latitude of the location and orientation facing due south.
- The PV modules operate at maximum power point during sunshine hours, with no shading considerations.
- An isotropic solar radiation model is considered.
- Additional system losses, which have been indicated in Table 3.

Table 3: System losses considered in solar PV output power modelling

Type of Loss	Value (in %)
Soiling loss	1
Mismatch loss	2
Conductor loss	5
Transformer loss	2
Net loss ( $N_L$ )	10

Solar radiation consists of three components, Global Horizontal Irradiance ( $GHI$ ), Direct Normal Irradiance ( $DNI$ ) and Direct Horizontal Irradiance ( $DHI$ ). The net effective radiation on a tilted solar module is required to calculate the power generated by the PV system, at a site. For this, we first estimated the solar angles and radiation tilt factors (Duffie & Beckman, 2013). The ground-reflected component of radiation is a function of the GHI and albedo factor ( $\rho$ ) of the surroundings (assumed as 0.2 in this analysis). The effective radiation on the tiled panel can be expressed as:

$$G_T = DNI * R_b + DHI * R_d + GHI * \rho * R_g$$

Where,

$G_T$  is the net effective solar radiation, incident on a tilted panel ( $W/m^2$ ),

$R_b$  is the module tilt factor for the beam component (DNI) of solar radiation,

$R_d$  is the module tilt factor for the diffused component (DHI) of solar radiation,

$R_g$  is the module tilt factor for the GHI of solar radiation,

$\rho$  is the albedo factor of the surrounding environment.

The performance of solar PV cells is sensitive to not only the incident solar radiation, but also the ambient temperature. On the other hand, the temperature of a solar cell ( $T_{cell}$ ) is dependent on, both, the ambient temperature and wind speeds, at a site. For this analysis, we considered a multi-crystalline silicon module (glass/cell/polymer sheet type) and a module mount of open rack configuration. We estimated the cell temperatures based on the specifications obtained from a referred report (King, Boyson, & Kratochvil, 2004). It can be expressed as:

$$T_{cell} = G_T * \exp(a_{CT} + b_{CT} * WS) + T_{amb} + (\Delta T) * G_T / G_{ref}$$

Where,

$a_{CT}$  is the empirically determined coefficient establishing the upper limit for module temperature at low wind speeds and high effective radiation on the panel,

$b_{CT}$  is the empirically determined coefficient establishing the rate at which the module temperature drops with an increase in the wind speed,

$T_{amb}$  is the ambient air temperature ( $^{\circ}\text{C}$ ),

$WS$  is the wind speed (m/s),

$\Delta T$  is the empirically determined temperature difference between the cell and module's back surface, at  $G_{ref} = 1,000 \text{ W/m}^2$  ( $^{\circ}\text{C}$ ),

$T_{cell}$  is the reference temperature ( $^{\circ}\text{C}$ ),

$G_{ref}$  is the reference solar radiation [ $1,000 \text{ W/m}^2$  at Standard Temperature Conditions (STC)] ( $\text{W/m}^2$ ).

The power generated by a solar PV module ( $P_M$ ) is computed by accounting for the effects of  $G_T$ ,  $T_{cell}$ , the specified power rating of the module [ $P_{module (STC)}$ ] and the temperature coefficient of power ( $K_T$ ), for a given module, as specified in the manufacturer's datasheet. The equation for calculating  $P_M$  has been specified in a referred report (Menicucci & Fernandez, 1988) and represented as:

$$P_M = P_{module (STC)} * (G_T / G_{ref}) * (1 + K_T * (T_{cell} - T_{ref}))$$

The power from one module ( $P_M$ ) is then multiplied with the total number of modules in the plant ( $N_{panels\_plant}$ ) to estimate the DC output of the entire PV plant, denoted as  $P_{pv}$ . A few additional losses, denoted as ( $N_L$ ), have also been accounted for, as shown in the following equation:

$$P_{pv} = N_{panels\_plant} * P_M * (1 - N_L)$$

## 3.2 Battery Storage Modelling

This section provides an overview of the performance modelling conducted for a lead-acid battery and its dispatch. This exercise helped us assess the battery charging/discharging power, for an instant, based on the modelled PV generation and input load demand data.

### 3.2.1 Overview of lead-acid battery model

The technical model of VRLA Absorbent Glass Mat (AGM) battery, used in this study, is based on the modelling work done by the System Advisor Model (SAM) of the National Renewable Energy Laboratory (NREL) (Diorio et al., 2015). We incorporated the concepts of a kinetic battery model to calculate the battery capacity, bound charge, available charge and State of Charge (SoC), for time-series calculations (Manwell & McGowan, 1993). The dynamic voltage model for batteries was used for voltage calculations (Diorio et al., 2015). The life-time estimation of a battery has been calculated based on a simple rain flow counting algorithm (Downing & Socie, 1982; Langella, Testa, & Ventre, 2014).

Figure 3 shows a block schematic overview of the battery model. The model provided outputs at, both, hourly and minute level time scales. The battery electrical model required inputs such as site demand and solar generation data, and user-defined battery capacity and voltage. In



addition, it also required battery-chemistry-specific voltage versus Depth of Discharge (DoD) characteristics, to model the battery voltage. The battery capacity fade profile was also included in the model to understand the decrease in a battery’s capacity when it is cycled at a certain DoD, and the maximum number of cycles that the battery can provide. The model provided outputs like the number of batteries that should be connected in series and parallel, based on the voltage and current requirement, and the dynamic change in battery current, voltage, power and SoC for the time period considered. In addition, we determined the battery life, in years, based on the cycling that the battery would undergo during dispatch. We plugged this calculated value into the financial model.

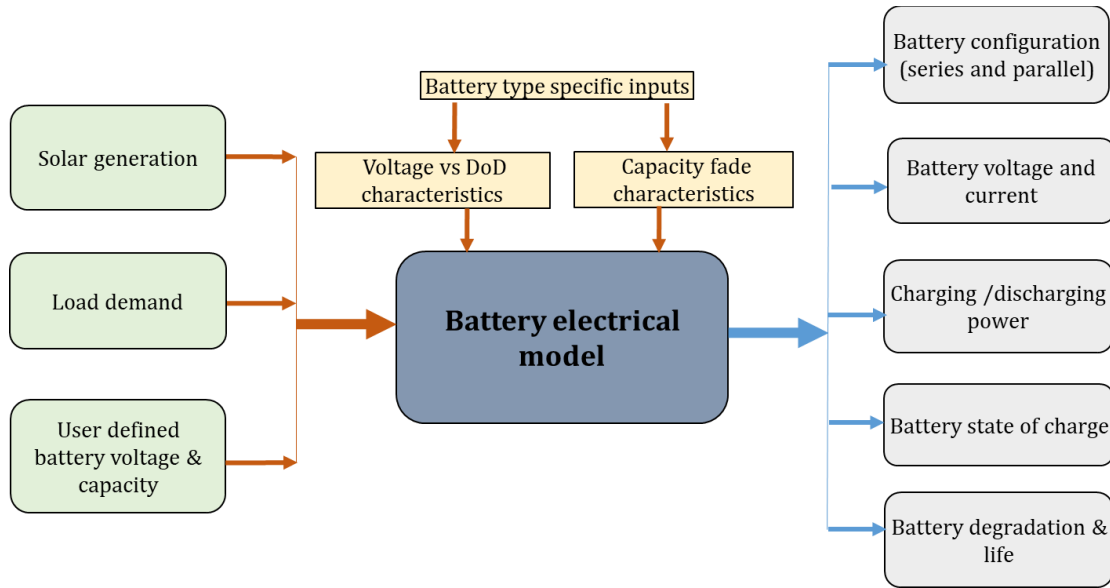


Figure 3: Block schematic for the lead-acid battery model

### Inputs for the battery model

Table 4 is a list of the technical specifications considered for the battery model. This includes important parameters like battery bank capacity and battery bank voltage, based on user input; battery cell properties; charge control parameters; and cell capacities at 1 hour, 10 hour and 20 hour rates. We have also included the conversion efficiencies of the inverter (DC to AC) and charge controller (DC to DC) in this Table, since they are intrinsic in the calculation for obtaining the accurate estimation of battery charging/discharging power.

Table 4: Inputs for the battery performance model

Parameter	Notation	Unit	Values
User-defined battery bank capacity	$BAT_s$	kWh	Input varied between 50 and 400
User-defined battery bank voltage	$V_{desired}$	V	48
Cell nominal voltage	$V_c$	V	2.0
Internal resistance	$R$	$\Omega$	0.1
C-rate of discharge curve	$C_d$	1/h	0.05
Fully charged cell voltage	$V_{full}$	V	2.2
Exponential zone cell voltage	$V_{exp}$	V	2.06
Nominal zone cell voltage	$V_{nom}$	V	2.03
Charge removed at exponential point	$q_{exp}$	%	0.25
Charge removed at nominal point	$q_{nom}$	%	90.0
Cell capacity	$q_c$	Ah	20
Maximum C-rate of charge	$C_{c,max}$	1/h	1.0

Maximum C-rate of discharge	$C_{d,max}$	1/h	1.0
Minimum state of charge	$SOC_{min}$	%	30
Maximum state of charge	$SOC_{max}$	%	95
DC to AC conversion efficiency	$\eta_{dcac}$	%	95
DC to DC conversion efficiency	$\eta_{dcdc}$	%	95
Ambient temperature	$T_a$	°C	20
Capacity at 1 hour rate	$q_{t=1}$	Ah	11.62
Capacity at 10 hour rate	$q_{t=10}$	Ah	18.7
Capacity at 20 hour rate	$q_{t=20}$	Ah	20.0
Time step	$\Delta t$	h	1.0

### 3.2.2 Design of the battery bank

In this section, we have discussed, in detail, the equations used to design the battery bank configuration for the parameters specified in Table 4 (NREL, 2017).

Number of cells in series ( $N_{series}$ ),

$$N_{series} = Integer \left( \frac{V_{desired}}{V_c} \right)$$

Capacity of one string ( $q_{1-string}$ ) in kWh,

$$q_{1-string} = \frac{N_{series} \times V_c \times q_c}{1,000}$$

Number of strings in parallel ( $N_{parallel}$ ),

$$N_{parallel} = Integer \left( \frac{BAT_s}{q_{1-string}} \right)$$

Actual bank capacity ( $q_{actual}$ ) in kWh,

$$q_{actual} = N_{parallel} \times q_{1-string}$$

Actual bank voltage ( $V_{actual}$ ) in V,

$$V_{actual} = N_{series} \times V_c$$

Maximum charge current ( $I_{c,max}$ ) in A,

$$I_{c,max} = \frac{C_{c,max} \times q_{actual} \times 1,000}{V_{actual}}$$

Maximum discharge current ( $I_{d,max}$ ) in A,

$$I_{d,max} = \frac{C_{d,max} \times q_{actual} \times 1,000}{V_{actual}}$$

Maximum power to charge the battery ( $P_{b,c,max}$ ) in kW,

$$P_{b,c,max} = q_{actual} \times C_{c,max}$$

Maximum discharge power ( $P_{b,d,max}$ ) in kW,

$$P_{b,d,max} = q_{actual} \times C_{d,max}$$

### 3.2.3 Battery dispatch strategy

We controlled the battery discharging schedules by developing a dispatch strategy. Since the size of a battery depends on its dispatch hours, we chose scenarios, with varying dispatch hours, to evaluate its effect on the battery size. Inputs for the dispatch model included:

- Dispatch time,  $t$  (hour or minute number)
- Load demand,  $P_{load}$
- Power output from PV,  $P_{pv}$
- Maximum power to charge the battery,  $P_{b,c,max}$
- Maximum power that can be discharged from the battery,  $P_{b,d,max}$

Table 5 shows three scenarios, which represent the change in duration of hours over which a battery is allowed to dispatch/discharge. For example, in Scenario 1, the battery was allowed to discharge anytime in a day when solar generation is unable to meet the demand. However, in Scenarios 2 and 3, battery discharge was allowed to commence only at a specified “dispatch time”—restricted to a certain number of hours.

Table 5: Battery dispatch Scenarios

Dispatch Scenarios	Dispatch Time	Hours of Battery Dispatch
Scenario 1	12 PM to 12 AM	24
Scenario 2	6 PM to 6 AM	12
Scenario 3	6 PM to 12 AM	6

To further illustrate the dispatch strategy, in Scenario 1, where the battery is allowed to discharge for 24 hours, we determined the battery power ( $P_b$ ) for time “ $t$ ”, using the following logic:

If ( $P_{pv} > P_{load}$ ),

$$P_b = -\text{Min}(|P_{load} - P_{pv}|, |P_{b,c,max}|), \text{ negative sign indicates charging power}$$

Else,

$$P_b = \text{Min}(|P_{load} - P_{pv}|, |P_{b,d,max}|), \text{ positive sign indicates discharging power}$$

Here,  $P_{b,c,max}$  and  $P_{b,d,max}$  were calculated as per the description provided in Section 3.2.2.

The logic described above indicates that in the three scenarios, the PV power output first supplies the load, before charging the battery. Appendix A.3 provides additional details of the lead-acid battery model. We extracted the SoC profile from the battery model to estimate the life of the battery. We then filtered the SoC data for a year, into distinct peaks and valleys, as shown in Figure 4, which is known as “filtered SoC” (Langella et al., 2014). Then, we used this filtered SoC as input in the rain flow counting algorithm (Downing & Socie, 1982) for battery life estimation. The filtered SoC helped in generating the number of cycles that elapsed during battery operation and the corresponding DoD. The battery life ( $L_b$ ) was estimated using the equation provided below:

$$L_b = \frac{1}{\sum_{i=1}^m \frac{N_i}{CF_i}}$$

Where,  $N_i$  is the number of cycles, with an average DoD of  $DOD_i$ , and  $CF_i$  is the maximum number of cycles that can be run. When the effective battery capacity degrades to 80% of the initial capacity, the battery is assumed to have reached its end of life (Diorio et al., 2015).

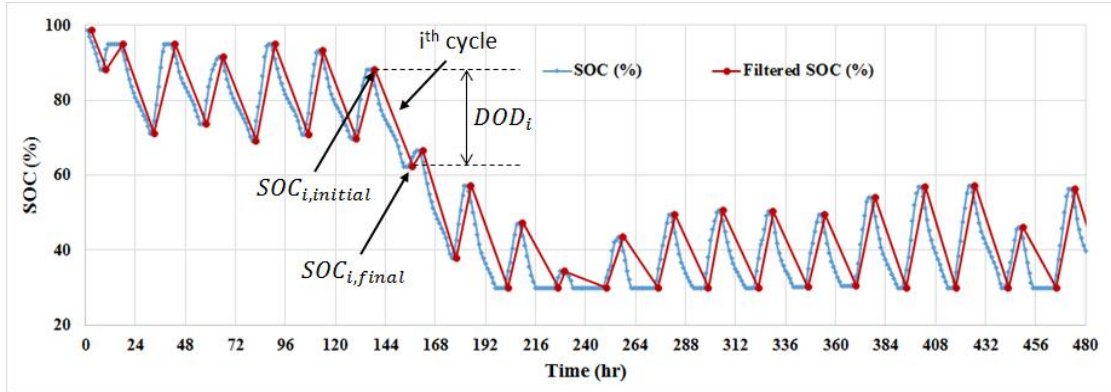


Figure 4: Sample SoC data and filtered SoC for rain flow counting algorithm

### 3.3 Technical Modelling for SPVMG

In Section 3.2.3, we have explained the dispatch logic for seamlessly combining the technical outputs from the PV and battery models. In order to complete the technical design of the SPVMG, the inverter has to be sized. We decided the inverter capacity based on the peak load demand for which the system was designed. As the inverter's output is directly connected to the load, as shown in Figure 1, the maximum power through the inverter, under normal operating conditions, will never exceed the peak demand for the site. Considering an additional safety margin of 25% above the peak demand, the inverter capacity, in kW, can be expressed as (Li, Zhu, Cao, Sui, & Hu, 2009):

$$INV_s = \frac{1.25 * Peak\ load\ demand}{Power\ Factor}$$

Since the peak load demand was 14 kW, we calculated the inverter size, in kVA, and rounded it off to be 20 kVA ( $1.25 * 14 / 0.9$ ). We assumed a power factor of 0.9 for the study.

To complete the technical modelling, the reliability outputs shown in Figure 2 were calculated.  $UL$  represents the fraction of load, which cannot be supplied by the SPVMG when the battery reaches  $SOC_{min}$  (lowest allowable SoC) during discharging.  $EX_{EL}$  represents the fraction of excess PV generation, which cannot be utilised for charging a battery when it reaches its maximum SoC ( $SOC_{max}$ ).  $T_{LPSP}$  is the probability of loss of power supply. It indicates the fraction of hours with no supply from either the PV or the battery, out of the total time instants in a year. These indicators are expressed below, in detail, for hourly calculations (8,760 is the total number of hours in a typical year):

$$UL = \frac{\sum_{i=1}^{8,760} Max \left\{ \left( \frac{P_{load}}{\eta_{acdc}} - P_{pv} \times \eta_{acdc} - P_b \right), 0 \right\}}{\sum_{i=1}^{8,760} (P_{load})}$$

$$EX_{EL} = \frac{\sum_{i=1}^{8,760} Max \left\{ \left( P_{pv} \times \eta_{acdc} - \frac{P_{load}}{\eta_{acdc}} - P_b \right), 0 \right\}}{\sum_{i=1}^{8,760} (P_{pv})}$$

$$T_{LPSP} = \frac{\text{Number of hours when } P_{pv} = 0 \text{ and } P_b = 0}{\text{Total number of hours in a year}}$$

The technical modelling for Scenario 1 has been mentioned below, as an example. We varied the PV size between 25 and 45 kW and the battery size between 50 and 400 kWh to provide several combinations of PV and battery coupling, as inputs to the model. We calculated the values of the reliability indicators from the model and recorded for all possible combinations of PV and battery sizes. A few combinations such as  $PV_s = 25$  kW,  $BAT_s = 50$  kWh or  $PV_s = 35$  kW,  $BAT_s = 95$  kWh are examples of inputs to the model. The load demand profile was kept constant across all scenarios. We maintained a constant inverter size of 20 kVA for all scenarios, considering it was designed for the input load profile.

### 3.4 Financial Modelling for SPVMG

We developed a financial model to determine the project cost and LCOE. To do so, we considered various fixed and operational costs incurred by micro-grid developers, under regular operating conditions. LCOE calculations were based on the method of the Central Electricity Regulatory Commission (CERC), to estimate electricity generation cost from renewable energy (RE) sources ("Draft CERC (Terms And Conditions For Tariff Determination From Renewable Energy Sources) Regulations, 2017 Central Electricity Regulatory Commission New Delhi," 2017).

The SPVMG component and installation costs shown in Table 6 are based on discussions with the Ministry of New and Renewable Energy (MNRE), a few component suppliers and micro-grid developers. The battery and inverter costs are based on prices quoted by MNRE's empanelled list of equipment manufacturers (MNRE, n.d.).

Table 6: Input system cost for a typical SPVMG

Component	Symbol	Cost	Unit
Module	$C_M$	25	INR/Wp
Solar Support Structure	$C_{SS}$	7	
Balance of System	$C_{BOS}$	10	
Transportation	$C_T$	3	
Civil & Electrical work	$C_{CE}$	7.5	
Distribution Network	$C_{DN}$	20	
Installation & Commissioning	$C_{IC}$	4	
Annual Operation and Maintenance (O&M)	$C_{O\&M}$	1.7	INR in lakhs
VRLA AGM Battery	$C_{BAT}$	8	INR/Wh
Inverter	$C_{INV}$	15	INR/VA

The annual Operation and Maintenance (O&M) cost ( $C_{O\&M}$ ) consists of the cost of employing two personnel to oversee the plant's O&M, collect tariff, maintenance, insurance and land lease costs. Table 7 shows the monthly cost for each of these expenses.

Table 7: O&M expenses

Monthly O&M Expenses	Values (INR)
Salary for two personnel	10,000
Maintenance	1,000
Land lease	2,000
Insurance	833
Total	13,833



The other parameters considered in the financial model were related to project life, debt and equity considerations, taxes and depreciation.

Table 8 lists these parameters and their values.

Table 8: Parameters for project finance

Parameter	Symbol	Value	Unit
Project Life	$P_L$	25	Years
Debt Component	$D_c$	70	%
Equity Component	$E_c$	30	%
Debt Interest Rate	$i$	10	%
Return on Equity Rate	$roe$	14	%
Pre Tax Discount Rate	$d$	11.2	%
Weighted Average Cost of Capital	$WACC$	8.8	%
Debt Repayment Period	$DRP$	13	Years
Annual Increase in O&M Costs	$O\&M_r$	5.72	%
Book Depreciation	$bd_r$	5.28 for first 13 years 1.78 for next 12 years	%
Corporate Tax Rate	$CR_r$	34.61	%
MAT Rate	$MAT_r$	19	%

Two parameters, crucial for understanding the project's financial details, were the Net Present Value (NPV) of the total system cost, denoted with  $NPV_{sys}$ , and  $LCOE$ .  $NPV_{sys}$  is the sum total of all the costs involved over the project life ( $P_L$ ), converted to present value by discounting the future cash flows by an appropriate discount factor ( $d$ ). It comprises cost of capital, total project O&M ( $O\&M_{val}$ ) and total depreciation ( $DEP_{val}$ ). The capital needed for such projects typically consist of debt ( $D_c$ ) and equity ( $E_c$ ) components. The cost associated with debt is represented as the total interest on term loan ( $INT_{val}$ ) and equity fraction is coined as the total return on equity ( $ROE_{val}$ ). Thus,  $NPV_{sys}$  is represented as:

$$NPV_{sys} = NPV(d, (O\&M_{val} + DEP_{val} + INT_{val} + ROE_{val}))$$

Appendix A.4 includes details of  $NPV_{sys}$  and  $LCOE$  calculations.

### 3.5 Techno-economic Modelling for SPVMG

We combined the capabilities of the technical and financial models with the objective of performing a techno-economic assessment of a SPVMG for a certain input demand profile and location. As shown in Figure 2, we varied the size of PV and battery ( $PV_s$  and  $BAT_s$ ) and used them as inputs to the dispatch model for a fixed load demand. For each combination of PV and battery size, we calculated the three reliability parameters from the technical model. We calculated the system costs and LCOE from the financial model for the same combination. This process was repeated for each of the three scenarios.

We eliminated systems showing greater than 50% unmet demand from the study, since their reliability was not deemed satisfactory. We then arranged the remaining system configurations from the lowest to highest value of LCOE and unmet demand for the three scenarios. Section 4.2 mentions the configurations providing the lowest LCOE and the lowest unmet demand (high reliability). Finally, we determined the best system size out of all the possible combinations by balancing cost and reliability.

## 4. Results and Discussion

In this section, we show the results for the performance of a typical SPVMG system, simulating its characteristics through our models. We found that the most suitable system configuration can be obtained by a trade-off between cost (LCOE) and system reliability. We found this by calculating both LCOE and unmet load for various combinations of PV and battery size. Since unmet load represents the fraction of demand not served, it is a direct indicator of system reliability.

### 4.1 Typical System Performance

Prior to describing the techno-economic analysis, we have presented the results associated with the performance of a SPVMG system, in this section. Figure 5 shows a set of six curves related to the hourly system performance, for a typical five-day period, for the year considered. The results have been shown for a sample system size of PV = 40 KW, Battery = 320 kWh and Inverter = 20 kVA, for 24 hours of unrestricted battery dispatch (Scenario 1). The hourly load and solar radiation data are inputs to the model. PV power and battery current [in Amperes (A)] were calculated from these inputs and determined the charging/discharging of the battery. The current is negative in charging mode and positive in discharging mode. The change in battery voltage [in Volts (V)], which has an inverse trend to current, is also captured in Figure 5. The hourly SoC profile indicates the fraction of battery capacity available at any point of time. The SoC increases while charging and decreases during discharging. The power to/from the battery (P to/fr Batt.) indicates the charging/ discharging power and has the same trend as current.

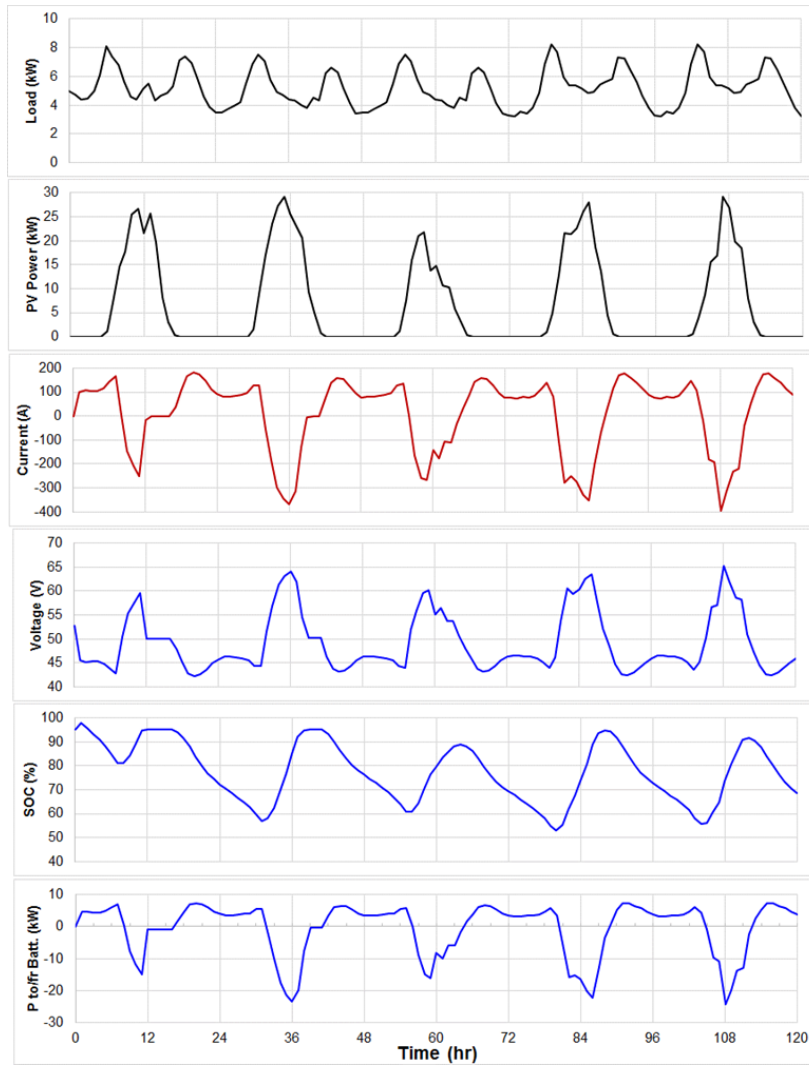


Figure 5: PV and battery performance characteristics over five typical days

Figure 6 (a) shows the variation in reliability indicators, namely  $EX_{EL}$ ,  $UL$  and  $T_{LPSP}$ , for a PV of size 35 kW and different battery capacities. In dispatch Scenario 1, with an increase in battery capacity,  $EX_{EL}$ ,  $UL$  and  $T_{LPSP}$  decrease significantly, up to 200 kWh, beyond which the decrease is marginal. A larger battery size, up to around 200 kWh in this case, helps meet the demand satisfactorily and limits the excess electricity. Figure 6 (b) shows the variation in battery life and average efficiency as functions of battery capacity. With an increase in battery capacity, for a fixed PV size, the life of the battery increases significantly, beyond 200 kWh. Batteries of higher sizes remain under-utilised and get cycled at low DoDs, which increases its life. The average efficiency of the battery decreases with increase in capacity, as the charging (input) power increases, for the same discharging (output) power, since demand does not change.

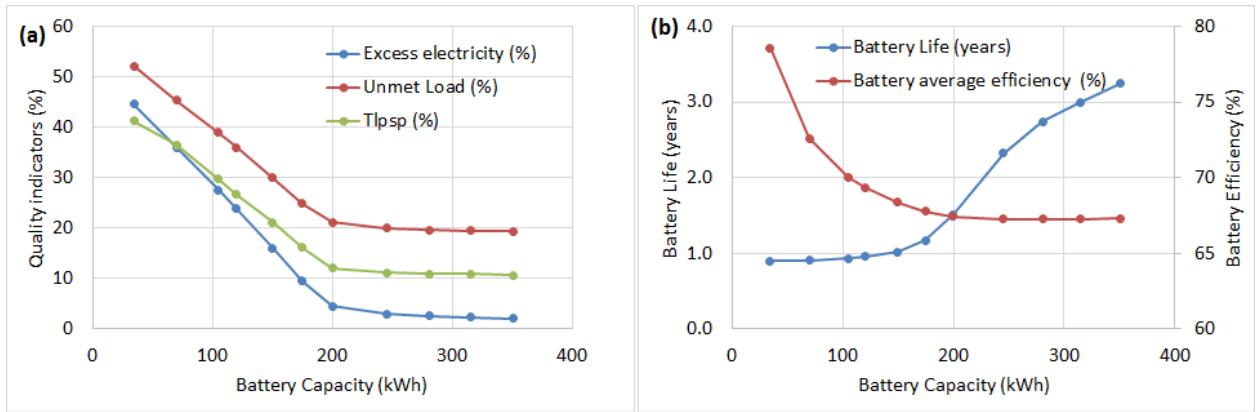


Figure 6: Variation in (a) reliability indicators and (b) battery life and efficiency for a 35 kW PV system

### 4.2 Scenarios for Feasibility Analysis

Figure 7 shows the percentage of unmet load for the three dispatch scenarios discussed in Section 3.2.3. We observed that a larger battery size improved its reliability by supplying the majority of the load. However, beyond a certain threshold of battery capacity, the fixed PV power (represented by individual trend lines) does not aid in improving reliability any further. We also saw that with higher PV size, system reliability improved in general. Moreover, we also observed that reliability in Scenario 3 was lower as compared to those in Scenarios 1 and 2 due to only 6 hours of battery discharge.

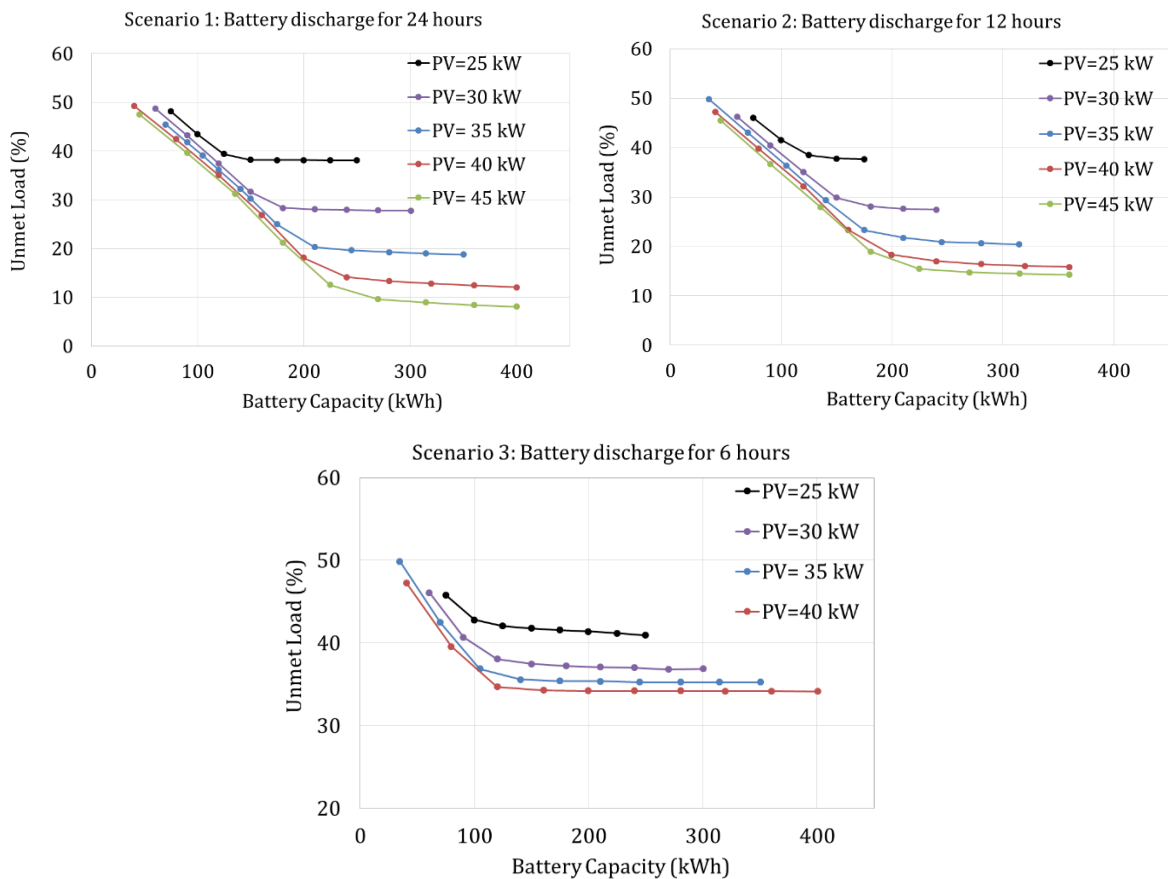


Figure 7: Scenarios 1-3 showing the variation in system unmet load

Figure 8 shows the variation in system LCOE corresponding to changes in the system size in all three scenarios. To evaluate systems from a cost perspective, we chose LCOE as it takes into

consideration the capital, replacement and operational costs involved in setting up a SPVMG. The LCOE trend showed that lower PV and battery sizes reduced the capital expenditure of the system and, in turn, lowered the LCOEs. However, the battery life increases with battery size (Figure 6, Scenario 2), thus fewer battery replacements are required. Hence, the lower battery replacement cost negates the increase in capital cost in some cases. Thus, the lowest values of LCOE for all three scenarios were found for systems with smaller PV sizes and battery size between 70 kWh and 150 kWh.

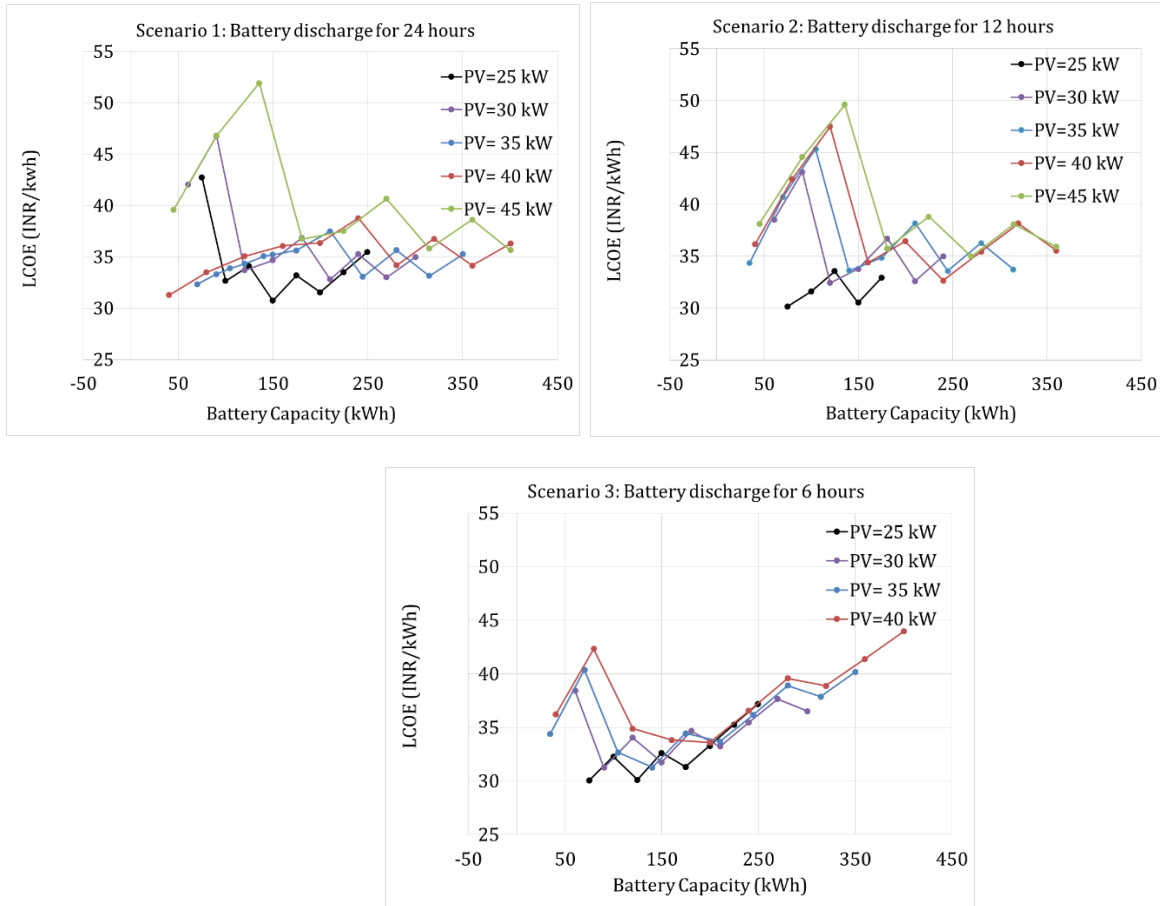


Figure 8: Variation in system LCOE for Scenarios 1-3

The results for Scenario 1 (as is evident from Figures 7 and 8) show that systems with lower PV and battery sizes provide lower LCOEs. However, these smaller capacity systems also have poor reliability (unmet load is typically greater than 30%). Scenarios 2 and 3 also show poor reliability, making it imperative to find pragmatic solutions and systems that are balanced in terms of cost and reliability. Table 9 lists the systems with the lowest LCOEs for each of the scenarios. We also evaluated the systems for reliability; those with the lowest unmet load are also listed.



Table 9: System configurations w.r.t. lower LCOE and higher reliability

Dispatch Scenarios	PV (kW)	Battery (kWh)	Inverter (kVA)	Unmet Load (%)	$T_{LPSP}$ (%)	Hours of Power Failure	LCOE (INR/kWh)	Battery Replacement (Year No.)
<b>Lowest LCOE</b>								
Scenario 1	25	150	20	38.2	27.1	6.5	30.7	3
Scenario 2	25	75	20	45.9	29.5	7.1	30.2	2
Scenario 3	25	75	20	45.8	30.2	7.3	30.0	2
<b>Lowest Unmet Load</b>								
Scenario 1	45	315	20	8.9	3.01	0.7	35.8	3
Scenario 2	45	270	20	14.8	5.5	1.3	34.9	3
Scenario 3	40	200	20	34.2	24.1	5.8	33.6	4

From the results shown above, it is evident that due to the limited number of hours of battery dispatch, the battery size requirement in Scenarios 3 and 2 were lesser than that in Scenario 1. The restriction on dispatch hours reduced the battery discharge time, allowing it to mostly charge from solar. This yielded systems with smaller battery sizes when evaluated for both, the lowest LCOE (due to reduction of expenditure on battery capital cost) and lowest unmet load. Scenario 3 provides a system with the lowest LCOE. However, reduction in the battery size also brings down the system reliability, which is observed as an increase in the percentage of unmet load and  $T_{LPSP}$ . This is mostly because of the unavailability of enough battery discharge power to meet the load.

Similarly, while narrowing down systems based on reliability, we found that Scenario 1 provides the best result as it had the lowest unmet load, indicating higher reliability. This is because the system size combination obtained in this case included large capacities of PV and battery, with 24 hours of battery dispatch allowed, meeting the demand satisfactorily. In Scenario 3, however, the unmet demand was as high as 34% even with 40 kW PV and 200 kWh battery. This was caused due to a limited discharge time of 6 hours only. Thus, a higher battery size would be required to bring down the unmet demand below 34%.

### Final “balanced” system configuration results

Once we evaluated the systems separately from the cost and reliability perspectives, we decided to select those configurations, which satisfy both these criteria reasonably. In order to do this, we looked at the other reliability indicator,  $T_{LPSP}$ , which shows the hours of power failure in a system for a user-defined combination of PV and battery size. We removed the systems showing greater than 3.5 hours of power failure in Scenarios 1 and 2. For Scenario 3, however, all the simulated system combinations showed more than 5 hours of power failure because of the limited battery discharge period. Thus, we eliminated the systems showing greater than 6 hours of power failure in Scenario 3 and chose a few system combinations with less probabilities of power failure. After filtering out the system sizes based on the constraints mentioned above, we sorted the remaining configurations from the smallest to largest LCOE.

Table 10 provides details of the combinations that provide the lowest LCOEs.

Table 10: System configurations obtained by trading-off both LCOE and unmet load

Dispatch Scenarios	PV (kW)	Battery (kWh)	Inverter (kVA)	Unmet Load (%)	T <sub>LPSP</sub> (%)	Hours of Power Failure	LCOE (INR/kWh)	Battery Replacement (Year No.)
Scenario 1	35	245	20	19.7	10.7	2.6	33.1	3
Scenario 2	30	210	20	27.6	12.9	3.1	32.5	3
Scenario 3	30	150	20	37.5	24.8	6.0	31.7	3

As indicated in Table 10, there is a significant reduction in battery size, from 245 kWh to 150 kWh while comparing Scenario 1 and Scenario 3. This is primarily due to the restricted battery discharge in Scenario 3. This increases the unmet load while lowering the LCOE due to a smaller battery size. We also observed that for Scenario 2, the battery size decreases by only 35 kWh, as compared to that in Scenario 1. The change is not very significant, considering battery discharging is usually limited to the night, on typical sunny days. In this sense, Scenario 2 is not very different from Scenario 1.

The reliability of power supply to load, however, decreases from Scenario 1 to 3 because of a decrease in system size. In Scenario 3, we notice 6 hours of power failure. Thus, a viable system configuration, which fares well in terms of both cost and reliability, is the one shown in Scenario 2, and is referred to as a “balanced” system. With a LCOE value that lies mid-way between those in the other two scenarios, this system of 35 kW PV and 210 kWh battery can supply power for around 21 hours (probable outage of around 3 hours), based on the load demand considered.

### 4.3 System Costs

We calculated the costs for the “balanced” system (Scenario 2 in Table 10) since it was the most promising in terms of both cost and reliability. Table 11–Table 13 show the total cost of the system and its break-up. Figure 9 to Figure 11 indicate the component-wise cost contributions to the system costs.

Table 11: Break-up of capital and fixed costs for the “balanced” system

Cost Component	Value (INR)
Capital cost	42,75,000
Fixed cost over plant life	1,49,88,317

Table 12: Break-up of capital cost for the “balanced” system

Cost Component	Value (INR)
PV module	7,50,000
Battery	16,80,000
Inverter	3,00,000
PV support structure	2,10,000
Balance of System	3,00,000
Transportation	90,000
Civil & Electrical	2,25,000
Distribution Network	6,00,000
Installation & Commissioning	1,20,000

Table 13: Break-up of fixed cost for the “balanced” system

Cost Component	Value (INR)
O&M	20,39,407
Present Value (P.V.) of Battery Replacement	41,29,033
P.V. of Inverter Replacement	1,39,665
Interest on Term Loan	24,41,222
Return on Equity	29,78,433
Depreciation	32,60,558

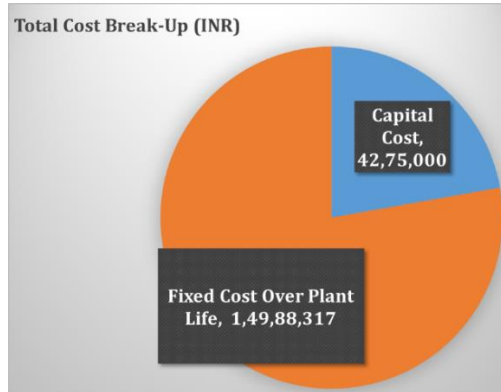


Figure 9: Break-up of capital cost and fixed cost for the “balanced” system

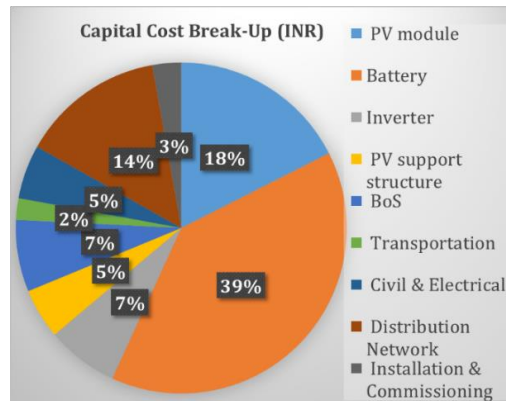


Figure 10: Break-up of capital cost for the “balanced” system

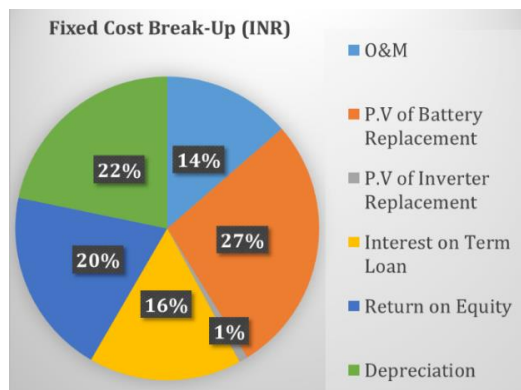


Figure 11: Break-up of fixed cost for the “balanced” system

## 4.4 Sensitivity Analysis

Since the system costs and LCOE are strong functions of input costs, we conducted a few sensitivity analyses on the “balanced” system to explore options for reducing the LCOE.

### 4.4.1 Capital cost as grant

Several micro-grid projects deployed in India till date have utilised CSR grants or similar funds to cover the capital cost of SPVMGs, thereby lowering the LCOE for a system developer, significantly. However, the fixed costs of the plant, comprising mostly plant O&M, cost of battery replacement and cost of inverter replacement, have to be recovered from electricity sale. For the “balanced” system, when the capital cost is provided as a grant, the LCOE works out to be INR 19.1/kWh. Table 14 shows the break-up of the system costs, when the capital cost is covered through a grant.

Table 14: Break-up of “balanced” system cost with grant based funding

Cost Component	Value (INR)
Capital Cost	0
Fixed cost over plant life	63,08,104

### 4.4.2 With VRLA Gel battery

We evaluated the “balanced” system (PV=30 kW, Battery=210 kWh) using the specifications of a different variant of lead-acid battery, namely the VRLA “Long life” Gel battery (Victron Energy, 2016). The capital cost of the battery increased by INR 1,500/kWh, as compared with that of the AGM variant. We conservatively assumed the life of the gel battery to be seven years, since the battery offers a design service life of maximum 10 years at 30°C. The LCOE for the same system reduced to INR 25.6/kWh. Table 15 shows the break-up of the system costs. Even though the capital cost is slightly higher, the fixed cost is nearly half of that shown in Table 11 for the same system using a VRLA AGM battery. Here, the fixed cost decreases due to fewer battery replacements while using a VRLA Gel battery.

Table 15: Break-up of “balanced” system cost using VRLA Gel battery

Cost Component	Value (INR)
Capital cost	45,90,000
Fixed cost over plant life	1,02,39,797

## 4.5 Techno-economic Comparison for Hourly and Minute-wise Simulations

We performed a techno-economic comparison of hourly and minute-wise simulations for the final shortlisted system configuration obtained in Scenario 2. Table 16 shows the results of the techno-economic comparison. We observed that the minute-wise simulations outperform the hourly simulations in capturing the granularity of battery performance. For the hourly modelling, two adjacent points represented two different hours. Thus, the change in battery charge/discharge power observed between two consecutive hours was significantly different as compared with that observed between consecutive minutes in the minute-scale modelling. This caused a considerable change in battery voltage in the hourly simulations. Thus, the battery losses calculated in the hourly simulations were also higher as opposed to those in the minute-level simulations. Unmet load and  $T_{LPSP}$  were higher in the hourly calculations as the smaller fluctuations went unnoticed. However, in the minute-wise simulations, the cycling of

battery closely resembles real operation. The battery undergoes frequent cycling and the calculated battery life is slightly lower than that in the hourly simulations. However, due to the lower value of battery losses, the net energy supplied from the SPVMG increased and hence LCOE was less in the case of the minute-wise simulations.

Table 16: Techno-economic comparison of hourly and minute-wise simulations for the “balanced” system

<b>Parameters</b>	<b>Hourly</b>	<b>Minute-wise</b>
Unmet load (%)	27.6	21.6
T <sub>L</sub> PSP (%)	12.9	7.1
Hours of power failure	3.1	1.7
Battery losses (kWh)	9,051.0	2,152.2
Battery replacement (in years)	2.6	2.1
LCOE (INR/kWh)	32.5	30.1

## 5. Policy Implications and Way Forward

This study helped us to evaluate the techno-economics of a SPVMG and determine a “balanced” system size. The key conclusions from the analysis are as follows:

- The LCOE for an off-grid SPVMG in KA ranges between INR 31–34/kWh.
- A “balanced” system is one where the battery dispatch is restricted to only 12 hours of operation (between 6 PM and 6 AM) and is well-balanced (low LCOE and high system reliability).
- This “balanced” system meets approximately 73% of the load demand and ensures an average of 21 hours of power supply per day.
- If a grant covers the capital cost of the “balanced” system, the LCOE decreases by about INR 13/kWh.
- The VRLA Gel battery has the potential to bring down the LCOE of the system by about INR 7/kWh.
- Serving 100% of the load with a standalone SPVMG is difficult and may warrant a drastic increase in system size, thus shooting up system costs.

The study showed that the cost of generating and supplying electricity through a SPVMG in rural areas will be higher than conventional electricity tariffs, which was approximately INR 4.1/kWh in 2015–16 (Prasad, 2017). This shows that in states like KA, such technologies could only be used when the cost of grid extension is higher than INR 34/kWh. Typically, the cost of grid extension varies depending on the region and may range between INR 3/kWh and approximately INR 200/kWh depending on the distance from the grid (Aggarwal et al., 2014). A SPVMG could be deployed only if the benefit of installing such a system outweighs the costs by a high margin.

The inherent design of a SPVMG offers very little scope for utilising the excess electricity generated. Exploring the idea of a grid-tied SPVMG, which allows the plant owner to export the excess electricity to the interconnected grid, would help him earn revenue for it. This would also provide the plant owner to increase the plant’s utilisation and reduce the dependency of the village on grid power.

To summarise, this study has brought forth an approach/methodology to conduct a techno-economic feasibility analysis for SPVMGs, for any location in India. If the inputs such as solar resource and load demand data are available, the models can easily be adapted. This robust approach could even be extended for analysing grid-tied SPVMGs, which can play a crucial role in improving the quality of power supply in electrified villages.

We examined three battery dispatch scenarios in this analysis; however, the approach provides a flexibility to evaluate additional scenarios as well. We performed a techno-economic comparison for the “balanced” system, at both hourly and minute-wise simulations, to understand battery behaviour in terms of its life and performance at different time scales. The results of the modelling activities revealed that the minute-wise simulation closely resembled the system operation and captured the granularity in battery dispatch better than the hourly calculations. Going forward, such studies could be carried out using higher resolution data, if available.



## References

- Aggarwal, V., Fahey, A., Freymiller, H. S., Li, S., Huang, C. C., & Moilanen, S. (2014). Rural Energy Alternatives in India : Opportunities in Financing and Community Engagement for Renewable Energy Microgrid Projects. *Princeton University's Woodrow Wilson School for Public and International Affairs*, 2, 1–66. Retrieved from: [https://www.princeton.edu/sites/default/files/content/591f Rural Energy Alternatives in India.pdf](https://www.princeton.edu/sites/default/files/content/591f_Rural_Energy_Alternatives_in_India.pdf)
- Diorio, N., Dobos, A., Janzou, S., Nelson, A., Lundstrom, B., Diorio, N., Lundstrom, B. (2015). Technoeconomic Modeling of Battery Energy Storage in SAM Technoeconomic Modeling of Battery Energy Storage in SAM, (September).
- Downing, S., & Socie, D. (1982). Simple rainflow counting algorithms. *International Journal of Fatigue*, 4(1), 31–40. [https://doi.org/10.1016/0142-1123\(82\)90018-4](https://doi.org/10.1016/0142-1123(82)90018-4)
- Draft CERC (Terms and Conditions for Tariff determination from Renewable Energy Sources) Regulations, 2017 Central Electricity Regulatory Commission New Delhi. (2017).
- Duffie, J. A., & Beckman, W. A. (2013). *Solar Engineering of Thermal Processes: Fourth Edition*. *Solar Engineering of Thermal Processes: Fourth Edition*. <https://doi.org/10.1002/9781118671603>
- Jain, A., Ray, S., Ganesan, K., Aklin, M., Cheng, C., & Urpelainen, J. (2015). Access to Clean Cooking Energy and Electricity. *ACEESS - Survey of States*, 1–98. <https://doi.org/10.7910/DVN/0NV9LF>
- King, D. L., Boyson, W. E., & Kratochvil, J. A. (2004). *Photovoltaic array performance model*. *Sandia Report No. 2004-3535*. <https://doi.org/10.2172/919131>
- Langella, R., Testa, A., & Ventre, C. (2014). A new model of lead-acid batteries lifetime in smart grid scenario (pp. 1343–1348). *IEEE*. <https://doi.org/10.1109/ENERGYCON.2014.6850597>
- Li, C.-H., Zhu, X.-J., Cao, G.-Y., Sui, S., & Hu, M.-R. (2009). Dynamic modeling and sizing optimization of stand-alone photovoltaic power systems using hybrid energy storage technology. *Renewable Energy*, 34(3), 815–826. <https://doi.org/10.1016/j.renene.2008.04.018>
- Manwell, J. F., & McGowan, J. G. (1993). Lead acid battery storage model for hybrid energy systems. *Solar Energy*, 50(5), 399–405. [https://doi.org/10.1016/0038-092X\(93\)90060-2](https://doi.org/10.1016/0038-092X(93)90060-2)
- Menicucci, D., & Fernandez, J. . (1988). *User's Manual for PVFORM: A Photovoltaic system simulation program for standalone and grid interactive applications*. Albuquerque, NM. <https://doi.org/SAND85-0376 UC-276>
- NREL. NREL's System Advisor Model (SAM) (2017).
- Victron Energy. (2016). Gel and AGM Batteries, 1–8. Retrieved from <http://www.victronenergy.com/>

## Appendix A

### A.1 Load Demand Data

For obtaining a continuous demand profile, we first aggregated month-wise data from feeder F6 for all the 12 months. From each month's data, we arranged the daily demand data in a matrix of size  $31 \times 1,440$ ,  $30 \times 1,440$  or  $28 \times 1,440$  depending on the month considered. In this case, 31, 30 or 28 indicated the number of days in a month and 1,440 represented the total minutes in a day. Then we calculated the mean of non-zero values for each day and replaced all the missing (or zero value) data points in a day. This process was repeated for all the days in a month and was completed for 12 months. The daily mean captured the average consumption in a day. We then arranged daily profiles to get a continuous demand profile, representing the electricity consumption for an entire year, at minute scale. We also generated an hourly demand profile from the same data. Subsequently, we used these two profiles as inputs for the technical modelling of a SPVMG.

We could not obtain information regarding the exact number of consumers corresponding to the demand profiles from the local distribution company serving Kollegal area in KA. We only had information that the feeder represented the electricity demand for close to 20 villages. Thus, we had to find a way of using this aggregated demand data. We conducted a demand estimation to calculate the peak day and night time demand of a typical village, as shown in Table 17 and Table A.1.2. We observed that the peak day and night time demand for a village comprising 120 households with domestic and other essential electricity needs were 9.5 kW and 12.8 kW, respectively, as shown in Table 17. The feeder demand data indicated a peak demand consumption of 1.4 MW. Thus, we scaled down the demand profile to 1% of its original value. This scaled-down profile had a peak demand of 14 kW, which is approximately close to the peak electricity demand (usually at night) seen in typical Indian villages comprising around 120 households, as shown in Table 17. While scaling down, we retained the intra-day variability in the demand profile to help design the system for a close-to-real demand pattern. Thus, the feeder load profile showed average and peak demands of 6.3 kW and 14 kW. We observed peak demand (14 kW) on April 6, 2015, for the time period considered. Therefore, we also looked at the demand pattern for the same day across different seasons to understand the variation in demand consumption across seasons. Figure 12 shows the hourly demand for four typical days of a year, i.e., 6<sup>th</sup> day of January, April, July and October.

Table 17: Use of electricity in a typical village in India

		Appliance	Numbers Used	Wattage/ Device	Total Watts
Household level		LED	2	5	10
		Mobile Charger	1	6	6
		Fan	1	40	40
		T.V	1	40	40
		Additional usage		20	20
Total consumption per house					116
Total domestic consumption for village					13,920
Community Level	Shop	LED	2	5	10
		Table Fan	1	20	20
	Streetlights	LED type	20	12	240
	Drinking water	Pump	1	1491.4	1491.4
	Irrigation	Pump	2	2237.1	4474.2
Estimated typical day time load	25% of household load+ 100 % pump load (drinking water and irrigation)				9,445.6
Estimated typical night time load	90% of household load+ 100 % community load (shops+ streetlights)				12,828

Table A.1.2: Categories of electricity use and their respective numbers in a village

Category	Numbers
Households	120
Shops	2
Streetlights	20
Pump for Drinking Water	1
Irrigation Pumps	2

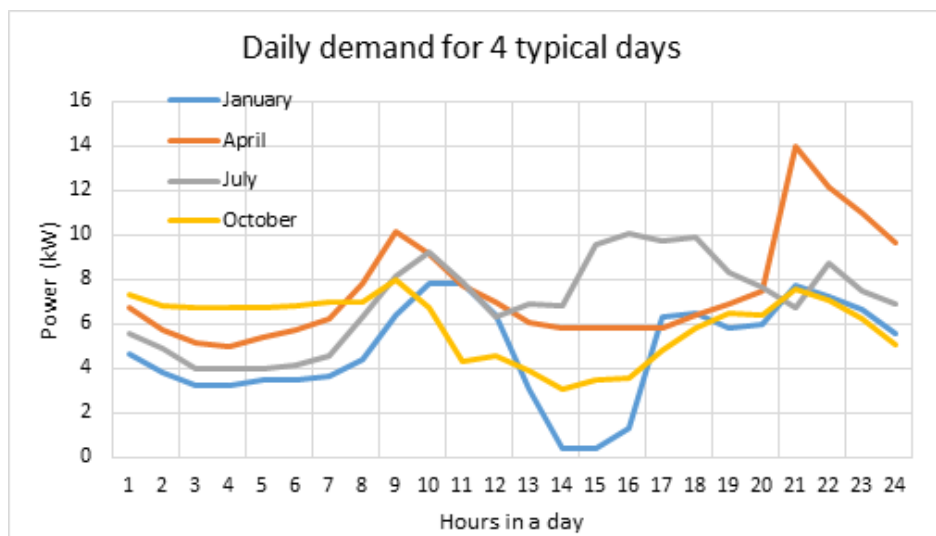


Figure 121: Typical load demand for representative days in four different months

## A.2 Solar Module Datasheet Parameters

Module manufacturer: ELDORA - Vikram Solar

Model name and mount type: Eldora VSP.72.320.03 - Multi-crystalline; Glass/Cell/Polymer sheet

Table 18: Solar PV module datasheet parameters

Parameter	Notation	Value
Voltage at maximum power point	$V_{mpp}$ (STC) (V)	38.4
Open-circuit voltage	$V_{oc}$ (STC) (V)	46.2
Short-circuit current	$I_{sc}$ (STC) (A)	8.95
Current at maximum power point	$I_{mpp}$ (STC) (A)	8.33
Power rating	$P_M$ (STC) (W)	320
Length of module	$L_{mod}$ (m)	0.982
Breadth of module	$B_{mod}$ (m)	1.955
Temperature coefficient of maximum power	%/C	-0.41
Temperature coefficient of open-circuit voltage	%/C	-0.31
Temperature coefficient of short-circuit current	%/C	0.052
Number of cells		72
Number of by-pass diodes		3

## A.3 Battery Performance Model

This section presents the details of the battery performance model. We modelled the performance characteristics based on the battery design, explained in Sections 3.2.1 and 3.2.2. The expressions used in determining the battery performance have been listed step-wise in this section.

Step-1: Calculate capacity ratio “ $c$ ”, rate constant “ $k$ ” and maximum cell capacity “ $q_{max,c}$ ” (Manwell & McGowan, 1993).

Step-2: Initialise the available charge,  $q_{1,0}$ , and bound charge,  $q_{2,0}$ , using the values of  $c$ :

$$q_{max,0} = q_{max,c} \times N_{parallel}$$

$$q_{1,0} = c \times q_{max,0}$$

$$q_{2,0} = (1 - c) \times q_{max,0}$$

Step-3: Initialise all variables required for the simulation

Step-4: Find the value of  $P_b$  at time “ $t$ ” as:

$$P_{b,c,max} = \text{Max} \left( \left( q_{max} - \frac{SOC_{max} q_{max,0}}{100} \right) V_{b,0} C_{c,max}, 0 \right)$$

$$P_{b,d,max} = \text{Max} \left( \left( q_{max} - \frac{SOC_{min} q_{max,0}}{100} \right) V_{b,0} C_{d,max}, 0 \right)$$

Step-5: If  $P_b > 0$ , battery will discharge power to the load. Compute  $I_d$ ,  $I_{d,max}$ ,  $q_{discharge}$ ,  $q_1$ ,  $q_2$ ,  $q$ ,  $V_c$ ,  $V_b$ ,  $SOC$ ,  $DOD$  and  $P_{from,battery}$ . The equations for computing the above parameters are as follows:

$$I_d = \left( \frac{P_b}{V_{b,0}} \right) / \eta_{dcac}$$

$$I_{d,max} = \frac{kq_{10}e^{-k\Delta t} + q_0kc(1 - e^{-k\Delta t})}{1 - e^{-k\Delta t} + c(k\Delta t - 1 + e^{-k\Delta t})}$$

$$I = \text{Min}(I_d, I_{d,max})$$

$$q_{discharge} = I\Delta t$$

$$q_1 = q_{1,0}e^{-k\Delta t} + \frac{(q_0kc - I) \times (1 - e^{-k\Delta t}) - Ic(k\Delta t - 1 + e^{-k\Delta t})}{k}$$

$$q_2 = q_{2,0}e^{-k\Delta t} + q_0(1 - c)(1 - e^{-k\Delta t}) - \frac{I(1 - c) \times (k\Delta t - 1 + e^{-k\Delta t})}{k}$$

$$q = q_1 + q_2$$

Calculate  $V_c$  from  $I$ ,  $q_0$ ,  $q$

$$V_b = V_c \times N_{parallel}$$

$$P_{frombattery} = \frac{(V_{b,0} + V_b)}{2} \times I \times \eta_{dcac}$$

$$SOC = 100 \times \frac{(q_{max} - q_{discharge})}{q_{max,0}}$$

$$DOD = 100 \times \frac{q_{discharge}}{q_{max,0}}$$

Step-6: In the same way, if  $P_b < 0$ , battery is in charging mode. Similarly, compute all parameters as follows:

$$I_c = \left( \frac{P_b}{V_{b,0}} \right)$$

$$I_{c,max} = \frac{-kcq_{max} + kcq_{max,0}e^{-k\Delta t} + q_{max,0}kc(1 - e^{-k\Delta t})}{1 - e^{-k\Delta t} + c(k\Delta t - 1 + e^{-k\Delta t})}$$

$$I = \text{Min}(I_c, I_{c,max})$$

$$q_{charge} = I\Delta t$$

$$P_{tobattery} = \frac{(V_{b,0} + V_b)}{2} \times I \times \eta_{dcac}$$

$SOC$  and  $DOD$  are calculated similarly to discharging mode.

Step-7: Calculate the reliability parameters: excess electricity, unmet load and  $T_{LPSP}$ :

$$P_{excess} = \text{Max} \left( P_{pv} \eta_{dcac} - \frac{P_{load}}{\eta_{dcac}} - |P_{tobattery}|, 0 \right)$$

$$P_{unmet} = \text{Max} \left( \frac{P_{load}}{\eta_{dcac}} - P_{pv} \eta_{dcac} - P_{frombattery}, 0 \right)$$

If ( $P_{pv} = 0$  &  $P_b = 0$ ), the value of  $T_{LPSP}$  increases by 1

$$T_{LPSP} = T_{LPSP} + 1$$

Step-8: Repeat the process and calculate the PV and battery output data for all 8,760 hours of the year.

#### A.4 Financial Model

This section covers the additional details regarding the methodology and expressions used in the financial modelling.

##### O&M calculation:

We denoted the O&M value for each year with  $C_{O\&M}$ ; the value for the first year was INR 1.66 lakh. The value of  $C_{O\&M}$  in year 1 was escalated at a rate of  $O\&M_r$ , annually, till the end of the project life ( $P_L$ ).

Thus,  $O\&M_{val}$  in the  $n^{\text{th}}$  year can be expressed as:

$$O\&M_{val,n} = \begin{cases} C_{O\&M}, & n = 1 \\ O\&M_{val,n-1} * (1 + \frac{O\&M_r}{100}), & 2 < n < 25 \end{cases}$$

Where,  $O\&M_{val,n-1}$  represents the value of O&M in the previous year.

##### Depreciation calculation:

$$DEP_{val} = NPV(d, DEP_{val,n})$$

We calculated the book depreciation value for a year, say “n”, as:

$$DEP_{val,n} = C_{SYS} * bd_r$$

The value of  $bd_r$  was 5.28% for the first 13 years and 1.78% for the next 12 years.

We calculated the total cost of the system,  $C_{SYS}$ , based on the system sizes obtained from the technical model. The expression for the total system cost is:

$$C_{SYS} = PV_s * (C_M + C_{SS} + C_{BOS} + C_T + C_{CCE} + C_{DN} + C_{IC}) + BAT_s * C_{BAT} + INV_s * C_{INV} + C_{BATr} + C_{INVR}$$

Where,  $C_{BATr}$  and  $C_{INVR}$  represent the total battery replacement cost and total inverter replacement cost, respectively, for a battery of size  $BAT_s$  and an inverter of size  $INV_s$ .



$C_{BATr} = NPV(d, BAT_s * C_{BAT})$ , with replacements occurring once in  $L_b$  years. We represented the battery life as  $L_b$  and calculated it from the technical model. If  $L_b$  is 3.4 years, for example, then to calculate the replacement cost, we rounded up  $L_b$  to the nearest integer, i.e., 4 years. Thus, the battery was replaced six times during a project life of 25 years.

We assumed the inverter to have a life of 10 years. Thus, it was replaced only twice in  $P_L$  years for all the simulated scenarios, and we calculated the total inverter replacement cost ( $C_{INVR}$ ) as:

$$C_{INVR} = NPV(d, INV_s * C_{INV})$$

#### Interest on term loan:

We calculated the interest on the term loan amount for the  $n^{\text{th}}$  year as:

$$INT_{val,n} = \frac{OB_n + CB_n}{2} * i$$

Where,  $OB_n$  is the opening balance and  $CB_n$  is the closing balance for  $n^{\text{th}}$  year:

$$OB_n = \begin{cases} D_c * C_{SYS}, & n = 1 \\ CB_n, & 2 < n < 13 \end{cases}$$

And,  $CB_n = OB_n - RP$  for  $1 < n < 13$ , where  $RP$  was the principal repayment for the  $n^{\text{th}}$  year and was continued for the Debt Repayment Period ( $DRP$ ) of 13 years:

$$RP = \frac{OB_{n=1}}{DRP}$$

#### Return on equity calculation:

We calculated the return on equity based on the equity component of the total cost of the system,  $C_{SYS}$ . It is expressed for the  $n^{\text{th}}$  year as:

$$ROE_{val,n} = E_c * C_{SYS} * roe$$

#### LCOE calculation:

LCOE is calculated as the ratio of the NPV of the total system cost ( $NPV_{SYS}$ ) and the NPV of the total electricity generated. It gives an indication of the cost of electricity generated from the SPVMG system by considering the entire lifecycle cost:

$$LCOE = \frac{NPV_{SYS}}{NPV(d, E_{gen})}$$

Here,  $E_{gen}$  represents the annual energy supplied to the load from the SPVMG system. This value shows the actual energy supplied after removing system losses, excess generation and the unmet demand in the system.







CENTER FOR STUDY OF SCIENCE, TECHNOLOGY AND POLICY

# 18 & 19, 10th Cross, Mayura Street,  
Papanna Layout, Nagashettyhalli, RMV II Stage,

Bengaluru - 560094

Karnataka, INDIA

Email: [cpe@cstep.in](mailto:cpe@cstep.in)

[www.cstep.in](http://www.cstep.in)